JACS
JOURNAL OF THE AMERICAN CHEMICAL SOCIETY

COMMUNICATION

pubs.acs.org/JACS

Enhanced Visible-Light Activity of Titania via Confinement inside Carbon Nanotubes

Wei Chen,*[,†] Zhongli Fan,[†] Bei Zhang,[‡] Guijun Ma,[†] Kazuhiro Takanabe,[†] Xixiang Zhang,[‡] and Zhiping Lai*[,†]

[†]Chemical and Life Sciences and Engineering Division and [‡]Imaging and Characterization Laboratory, King Abdullah University of Science and Technology, Thuwal, Kingdom of Saudi Arabia

Supporting Information

ABSTRACT: Titania confined inside carbon nanotubes (CNTs) was synthesized using a restrained hydrolysis method. Raman spectra and magnetic measurements using a SQUID magnetometer suggested the formation of remarkable oxygen vacancies over the encapsulated TiO_2 in comparison with nanoparticles dispersed on the outer surface of CNTs, extending the photoresponse of TiO_2 from the UV to the visible-light region. The CNT-confined TiO_2 exhibited improved visible-light activity in the degradation of methylene blue (MB) relative to the outside titania and commercial P25, which is attributed to the modification of the electronic structure of TiO_2 induced by the unique confinement inside CNTs. These results provide further insight into the effect of confinement within CNTs, and the composites are expected to be promising for applications in visible-light photocatalysis.

TiO_2 has long been a promising candidate for photocatalysis applications because of its photostability, natural abundance, and nontoxicity.[1] Because of its limitation to UV-light response, extensive efforts to modify the electronic band structures of TiO_2 for visible-light harvesting are being conducted, including metal/nonmetal doping, coupling with secondary semiconductors, and photosensitization with dyes.[2−5] Among these, composites of TiO_2 supported by nanoscale carbonaceous materials have drawn much attention in recent years,[6−8] by virtue of their ability to extend the light-response range and other distinctive features such as facile charge separation and increased adsorption of pollutants. In comparison with other nanocarbon materials, carbon nanotubes (CNTs) are distinguished in that they possess tubular morphologies with graphene layers.[9] It has been reported that the well-defined nanochannels of CNTs with unique electronic tuning properties can provide an intriguing confinement environment.[10] Significantly enhanced catalytic activities have been observed over CNT-confined catalysts as a result of tuning the properties of active species via confinement inside CNTs.[11−14] However, few studies of the applications of TiO_2 encapsulated within CNTs in photocatalysis have been reported.[15] To date, it is still a great challenge to disperse TiO_2 nanoparticles uniformly inside CNTs because of rapid hydrolysis of the titanium precursors. Here we developed an efficient method for synthesizing TiO_2 encapsulated within CNTs by restrained hydrolysis of the titanium precursor. The as-prepared CNT-confined TiO_2 composites showed high visible-light photoactivity resulting from the modification of electronic properties of TiO_2 particles induced by the unique confinement inside CNTs.

Titania nanoparticles were introduced into the CNT channels with titanium isopropoxide as the precursor under a N_2 atmosphere using the capillary force of the tubes, by which the sample denoted as TC-*in* was obtained [section SI1 in the Supporting Information (SI)]. For comparison, particles with the same composition were dispersed on the outer surface of CNTs, affording the sample denoted as TC-*out*. Transmission electron microscopy (TEM) investigations revealed that most of the particles were neatly aligned in the channels for the TC-*in* sample and that almost all of the particles were located outside CNTs in TC-*out* (Figure 1a,b and Figure S1 in the SI). Particles with *d* spacing of 3.52 Å, corresponding to the [101] lattice fringe of anatase TiO_2, were observed in TC-*in* and TC-*out*, indicating that the titania nanoparticles were in an anatase phase. Size distribution diagrams showed that over 85% of the TiO_2 particles in both TC-*in* and TC-*out* had sizes in the range 3−8 nm. The scanning electron microscopy (SEM) image in Figure 1c shows that in reference TiO_2 particles (prepared using the same process but without CNTs; see section SI1) were fairly homogeneous with a much narrower particle size distribution (7−12 nm) relative to commercial P25, which had sizes in the range 15−32 nm (Figure 1d). This implies that uniform TiO_2 nanoparticles were successfully obtained by the restrained hydrolysis method.

X-ray diffraction (XRD) patterns of TC-*in* and TC-*out* are displayed in Figure 2a,b. The diffraction peaks corresponding to anatase TiO_2 [004], [200], [211], [204], [220], and [215] planes (JCPDS no. 21-1272, marked with triangles) were detected along with the characteristic features of CNTs. In addition, the most intense peak from anatase TiO_2 [101] overlapped with that of CNT [002]. No diffraction peaks from the rutile phase were observed. This demonstrates that the titania nanoparticles in both TC-*in* and TC-*out* existed in an anatase state, in agreement with the TEM results. Figure 2c shows the XRD pattern of reference TiO_2, and all of the peaks matched the standard spectra of anatase TiO_2 well. Commercial P25 (Figure 2d) possessed peaks from both anatase and rutile phases (marked with diamonds), as recognized previously.[16] The particle sizes of reference TiO_2 and P25 were 10.5 and 22.0 nm, respectively, as calculated using the Scherrer equation on the basis of the anatase [200] peak. In comparison with reference TiO_2 and P25, the peaks of TiO_2 supported on CNTs either inside or outside the

Received: June 28, 2011
Published: September 06, 2011

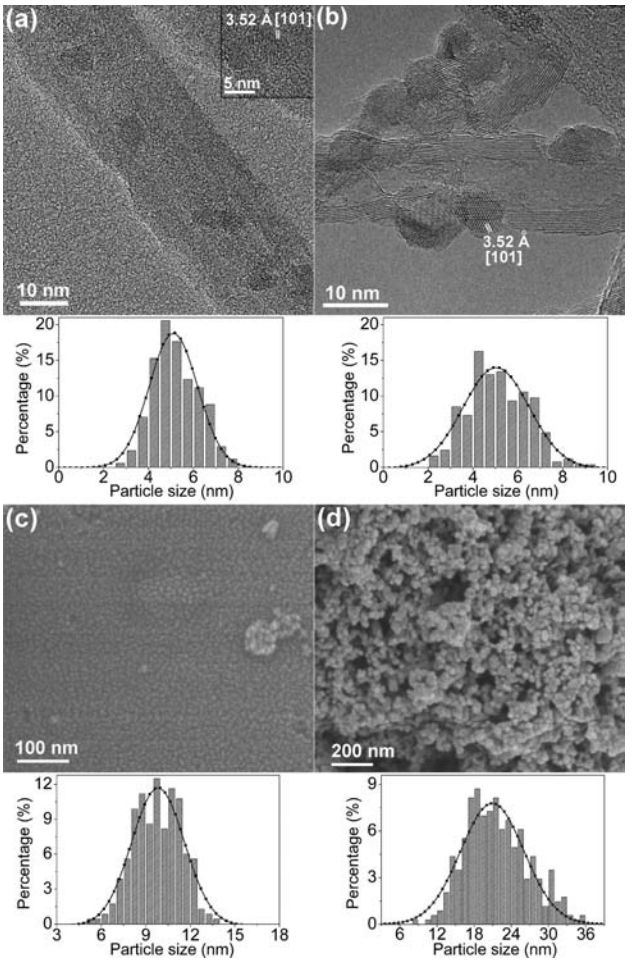

Figure 1. (a, b) TEM and (c, d) SEM images and size distributions of TiO_2 nanoparticles in (a) TC-*in*, (b) TC-*out*, (c) reference TiO_2, and (d) P25.

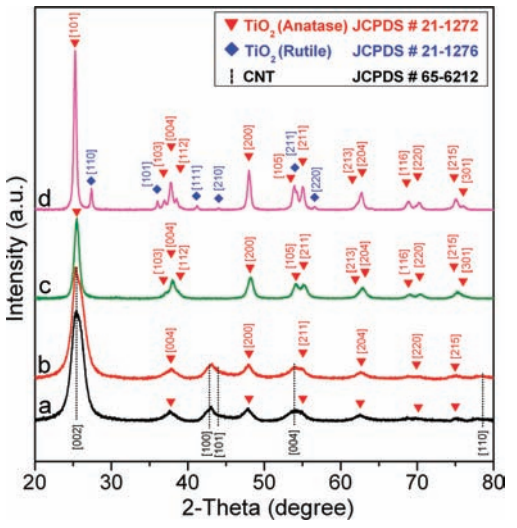

Figure 2. XRD patterns of (a) TC-*in*, (b) TC-*out*, (c) reference TiO_2, and (d) P25.

channels were greatly broadened. The average crystal size of TiO_2 in TC-*in* was ~4.6 nm, which is close to that of TC-*out* (5.3 nm). These results agree well with the microscopy observations in Figure 1.

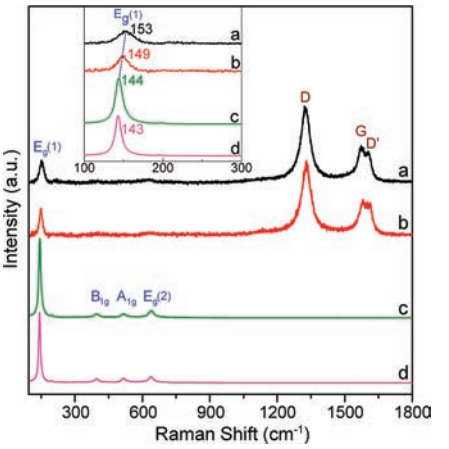

Figure 3. Raman spectra of (a) TC-*in*, (b) TC-*out*, (c) reference TiO_2, and (d) P25.

In the Raman spectra, both TC-*in* and TC-*out* exhibited three bands in the high-frequency region corresponding to the characteristic CNT D, G, and D′ modes.[17] Below 1000 cm^{-1}, a sharp peak at ~150 cm^{-1} and a broad one at ~630 cm^{-1} were also detected (Figure 3a,b). These bands can be assigned to the $E_g(1)$ and $E_g(2)$ modes of the Ti(IV)−O bond vibration in anatase TiO_2,[18] as manifested by the similar Raman bands in reference TiO_2 (Figure 3c). The Raman peaks of P25 (Figure 3d) were very close to those of reference TiO_2, indicating that the surface of P25 was in an anatase state.[19]

The $E_g(1)$ feature of the Ti−O band was studied in detail (Figure 3 inset). Although the particle sizes of reference TiO_2 (10.5 nm) and P25 (22.0 nm) were quite different, their Ti−O vibrations exhibited almost same ν_{Ti-O} frequency, implying that a particle size dependence of the Raman shift is ruled out in the current case, in agreement with the results of earlier reports.[20,21] However, the $E_g(1)$ mode of Ti−O in the spectrum of TC-*in* (153 cm^{-1}) was upshifted by 4 cm^{-1} relative to that of TiO_2 on the outer surface of CNTs (149 cm^{-1}), which is similar to the phenomenon reported previously for Fe_2O_3 confined within CNTs.[22] We ascribe the upshift of the ν_{Ti-O} $E_g(1)$ mode to the unique interaction between the TiO_2 nanoparticles and the CNT inner walls. It is known that because of the deviation from planarity, the π-electron density of CNTs is not evenly distributed, with the interior surface being relatively electron-deficient in comparison with the outer surface.[23,24] Thus, TiO_2 particles interact with the interior walls differently than with the exterior walls. Within the CNTs, attracting the anionic oxygen in TiO_2 can partially compensate for the loss of electron density, leading to distortion of the TiO_2 crystal lattice and the formation of nonstoichiometric oxygen vacancies in the asymmetric TiO_2. Such oxygen vacancies in titania crystals has been suggested to be responsible for the $\nu_{Ti(IV)-O}$ shifts toward high frequency.[25,26]

Since there are unpaired electrons in the structure of the oxygen vacancies in the TiO_2 crystal,[27,28] we investigated the titania by superconducting quantum interference device (SQUID) measurements in order to gain further insight into the electronic structure of titania confined inside CNTs. Figure 4 illustrates the specific-mass magnetization (M) of the samples as a function of the applied magnetic field measured up to ±50 kOe at 5 K. The

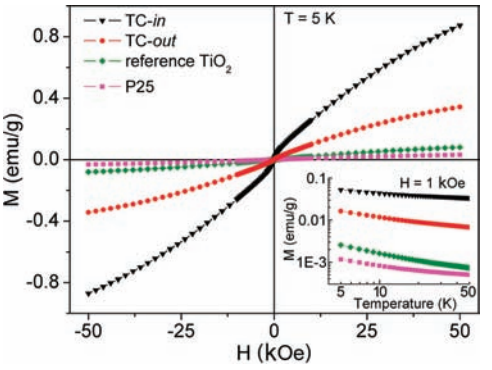

Figure 4. Magnetization curves for TC-*in*, TC-*out*, reference TiO_2, and P25 measured under external magnetic fields (H) from −50 to 50 kOe at T = 5 K. The temperature-dependent magnetizations measured under a constant magnetic field of 1 kOe from 5 to 50 K are shown in the inset.

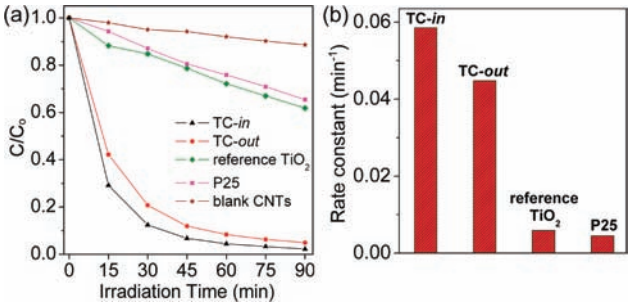

Figure 5. (a) MB degradation curves vs irradiation time under visible-light irradiation ($\lambda \geq 420$ nm). (b) Average reaction rate constants k for photodegradation of MB over TC-*in*, TC-*out*, reference TiO_2, and P25.

contribution from blank CNTs is negligible under the same conditions (see section SI2). Both TC-*in* and TC-*out* exhibited apparently paramagnetic behavior, and the M values at 50 kOe and 5 K were estimated as 0.9 and 0.35 emu/g, respectively; the M values of reference TiO_2 and commercial P25 were much smaller (<0.1 emu/g at 50 kOe, 5 K). The Figure 4 inset shows that the M values of TC-*in* and TC-*out* were larger than those of reference TiO_2 and P25 from 5 to 50 K. This implies a quite large amount of unpaired electrons in the titania of TC-*in* and TC-*out*, which possibly arise from oxygen vacancies.[28] Notably, the M value of TC-*in* was 2.57 times that of TC-*out*, indicating that the formation of oxygen vacancies is likely facilitated for the titania confined inside CNTs in comparison with the outside ones. It is known that the emergence of oxygen vacancies results in reduced TiO_2 (TiO_{2-x}, i.e., Ti^{3+} species).[28] The CNT-confined environment is reported to be inclined to retain reduced oxidation states for transition-metal oxides because of the electronic interaction of the confined metal oxides with the inner surface of CNTs.[13] Thus, the CNT-confined titania particles can more easily form lower-oxidation-state species such as Ti^{3+} with oxygen vacancies in comparison with exterior particles, which is consistent with the Raman results.

The photocatalytic activities of TC-*in* and TC-*out* were evaluated using the photodegradation of methylene blue (MB) under visible-light irradiation ($\lambda \geq 420$ nm) as a probe reaction, and the results are shown in Figure 5. The value of (C/C_o), the instantaneous concentration of MB during the photodegradation normalized to the initial concentration C_o, was proportional to the normalized maximum absorbance (A/A_o), which was measured at λ = 664 nm at regular time intervals (see section SI3). It can be seen that ~70 and ~60% of the initial dye was decomposed by TC-*in* and TC-*out*, respectively, after 15 min (Figure 5 a). After 90 min of irradiation, only 2.2 and 4.9% of the initial dye remained in the solution for TC-*in* and TC-*out*. In contrast, nearly 62 and 65% of the initial dye still remained after 90 min for reference TiO_2 and P25. In addition, blank CNTs showed little photocatalytic activity. The kinetics of the degradation reaction were fitted to a pseudo-first-order rate law at low dye concentration using the equation $\ln(C_o/C) = kt$, where k is the apparent rate constant and t is the irradiation time.[29] From Figure 5b, one can see that the average values of k for TC-*in* and TC-*out* were 0.0585 and 0.0448 min^{-1}, respectively, which were ~10 times those of bare TiO_2 (reference TiO_2, k = 0.0059 min^{-1}; P25, k = 0.0045 min^{-1}). Furthermore, we note that the activity of TC-*in* was 31% higher than that of TC-*out*, although diffusion of MB molecules in and out of the CNT channels might hinder the reaction to some degree in comparison with that on the freely accessible outer CNT surface. It has been reported that oxygen vacancies or Ti^{3+} could extend the photoresponse of TiO_2 from the UV to the visible-light region.[30−32] Profiting from the confinement environment within CNTs, the formation of Ti^{3+} or oxygen vacancies is facilitated in titania encapsulated inside CNTs, as evidenced by the Raman and magnetization measurements. Thus, TC-*in* exhibits a higher activity in the photodegradation of MB than TC-*out*, reference TiO_2, and P25 under visible-light irradiation.

In summary, the CNT-confined TiO_2 catalyst demonstrated significant advancement over titania on the outer surface of CNTs, reference TiO_2, and commercial P25 in the photodegradation of MB under visible-light irradiation. Raman spectra and magnetic measurements supported the hypothesis that it is Ti^{3+} or oxygen vacancies generated from the modified electronic structure of TiO_2 via the confinement inside CNTs that accounts for the extension of the photocatalytic activity from the UV to the visible-light region. The present study provides a facile and economical approach for tuning the band gap of TiO_2 and developing highly active photocatalysts to expand their applications to environmental remediation and solar energy utilization.

■ ASSOCIATED CONTENT

Supporting Information. Detailed sample preparation; additional characterization details; magnetization measurements; photocatalytic activity tests. This material is available free of charge via the Internet at http://pubs.acs.org.

■ AUTHOR INFORMATION

Corresponding Author
wei.chen.1@kaust.edu.sa; zhiping.lai@kaust.edu.sa

■ ACKNOWLEDGMENT

We thank Dr. Y. Yang, Q. Wang, and X. Liu from King Abdullah University of Science and Technology (KAUST) for their help with Raman spectroscopy, TEM, and drawing, respectively. We also acknowledge the faculty distribution fund of KAUST.

■ REFERENCES

(1) Fujishima, A.; Honda, K. *Nature* **1972**, *238*, 37.

(2) Choi, W.; Termin, A.; Hoffmann, M. R. *J. Phys. Chem.* **1994**, *98*, 13669.
(3) Chen, X.; Burda, C. *J. Am. Chem. Soc.* **2008**, *130*, 5018.
(4) Tada, H.; Mitsui, T.; Kiyonaga, T.; Akita, T.; Tanaka, K. *Nat. Mater.* **2006**, *5*, 782.
(5) Reisner, E.; Powell, D. J.; Cavazza, C.; Fontecilla-Camps, J. C.; Armstrong, F. A. *J. Am. Chem. Soc.* **2009**, *131*, 18457.
(6) Zhang, H.; Lv, X.; Li, Y.; Wang, Y.; Li, J. *ACS Nano* **2010**, *4*, 380.
(7) (a) Woan, K.; Pyrgiotakis, G.; Sigmund, W. *Adv. Mater.* **2009**, *21*, 2233. (b) Dai, K.; Peng, T.; Ke, D.; Wei, B. *Nanotechnology* **2009**, *20*, No. 125603. (c) Eder, D.; Windle, A. H. *Adv. Mater.* **2008**, *20*, 1787. (d) Lu, S.-Y.; Tang, C.-W.; Lin, Y.-H.; Kuo, H.-F.; Lai, Y.-C.; Tsai, M.-Y.; Ouyang, H.; Hsu, W.-K. *Appl. Phys. Lett.* **2010**, *96*, No. 231915.
(8) Leary, R.; Westwood, A. *Carbon* **2011**, *49*, 741.
(9) Ajayan, P. M. *Chem. Rev.* **1999**, *99*, 1787.
(10) Pan, X.; Bao, X. *Chem. Commun.* **2008**, 6271.
(11) Castillejos, E.; Debouttiere, P. J.; Roiban, L.; Solhy, A.; Martinez, V.; Kihn, Y.; Ersen, O.; Philippot, K.; Chaudret, B.; Serp, P. *Angew. Chem., Int. Ed.* **2009**, *48*, 2529.
(12) Pan, X.; Fan, Z.; Chen, W.; Ding, Y.; Luo, H.; Bao, X. *Nat. Mater.* **2007**, *6*, 507.
(13) Chen, W.; Fan, Z.; Pan, X.; Bao, X. *J. Am. Chem. Soc.* **2008**, *130*, 9414.
(14) Zhang, H.; Pan, X.; Liu, J.; Qian, W.; Wei, F.; Huang, Y.; Bao, X. *ChemSusChem* **2011**, *4*, 975.
(15) Oh, W. C.; Zhang, F. J.; Lim, C. S.; Chen, M. L. *J. Ceram. Process. Res.* **2010**, *11*, 479.
(16) Zhang, L. W.; Fu, H. B.; Zhu, Y. F. *Adv. Funct. Mater.* **2008**, *18*, 2180.
(17) Eklund, P. C.; Holden, J. M.; Jishi, R. A. *Carbon* **1995**, *33*, 959.
(18) Ohsaka, T.; Izumi, F.; Fujiki, Y. *J. Raman Spectrosc.* **1978**, *7*, 321.
(19) Su, W.; Zhang, J.; Feng, Z.; Chen, T.; Ying, P.; Li, C. *J. Phys. Chem. C* **2008**, *112*, 7710.
(20) Parker, J. C.; Siegel, R. W. *Appl. Phys. Lett.* **1990**, *57*, 943.
(21) Xie, Y.; Heo, S. H.; Yoo, S. H.; Ali, G.; Cho, S. O. *Nanoscale Res. Lett.* **2010**, *5*, 603.
(22) Chen, W.; Pan, X.; Bao, X. *J. Am. Chem. Soc.* **2007**, *129*, 7421.
(23) Haddon, R. C. *Science* **1993**, *261*, 1545.
(24) Ugarte, D.; Chatelain, A.; de Heer, W. A. *Science* **1996**, *274*, 1897.
(25) Parker, J. C.; Siegel, R. W. *J. Mater. Res.* **1990**, *5*, 1246.
(26) Bassi, A. L.; Cattaneo, D.; Russo, V.; Bottani, C. E.; Barborini, E.; Mazza, T.; Piseri, P.; Milani, P.; Ernst, F. O.; Wegner, K.; Pratsinis, S. E. *J. Appl. Phys.* **2005**, *98*, No. 074305.
(27) Vettraino, M.; Trudeau, M.; Antonelli, D. M. *Inorg. Chem.* **2001**, *40*, 2088.
(28) Liu, H.; Ma, H. T.; Li, X. Z.; Li, W. Z.; Wu, M.; Bao, X. H. *Chemosphere* **2003**, *50*, 39.
(29) Wang, X. H.; Li, J. G.; Kamiyama, H.; Moriyoshi, Y.; Ishigaki, T. *J. Phys. Chem. B* **2006**, *110*, 6804.
(30) Zuo, F.; Wang, L.; Wu, T.; Zhang, Z.; Borchardt, D.; Feng, P. *J. Am. Chem. Soc.* **2010**, *132*, 11856.
(31) Nakamura, I.; Negishi, N.; Kutsuna, S.; Ihara, T.; Sugihara, S.; Takeuchi, K. *J. Mol. Catal. A: Chem.* **2000**, *161*, 205.
(32) Justicia, I.; Ordejon, P.; Canto, G.; Mozos, J. L.; Fraxedas, J.; Battiston, G. A.; Gerbasi, R.; Figueras, A. *Adv. Mater.* **2002**, *14*, 1399.